

Time series versus argument of latitude

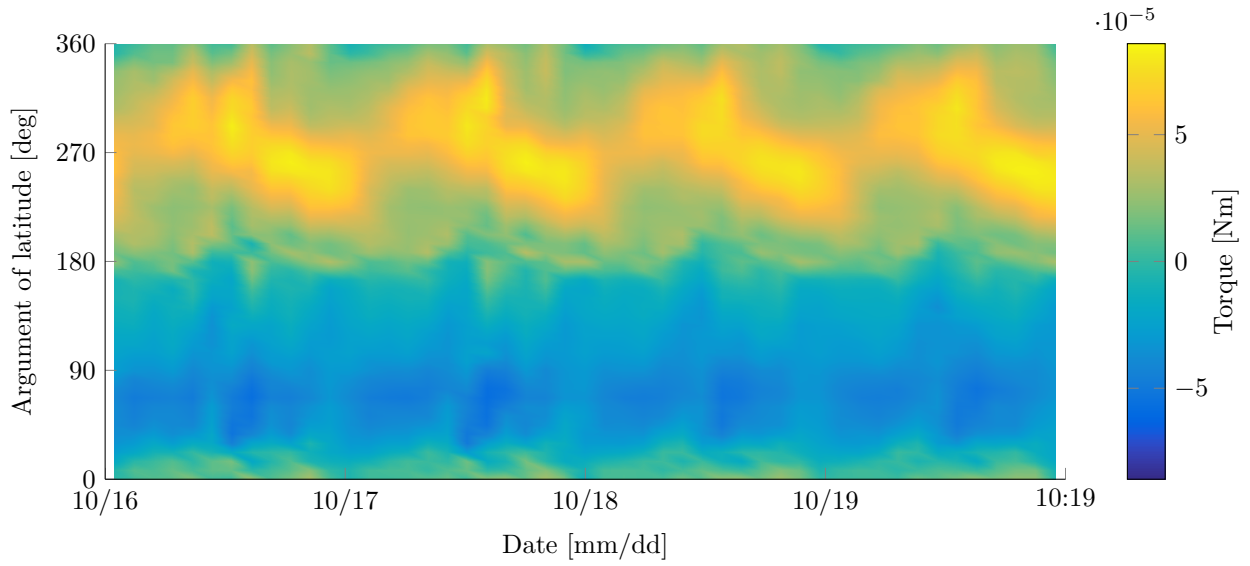
GOCE Aerodynamic Torque Modeling

T. Visser, E.N. Doornbos, C.C. de Visser, P.N.A.M. Visser

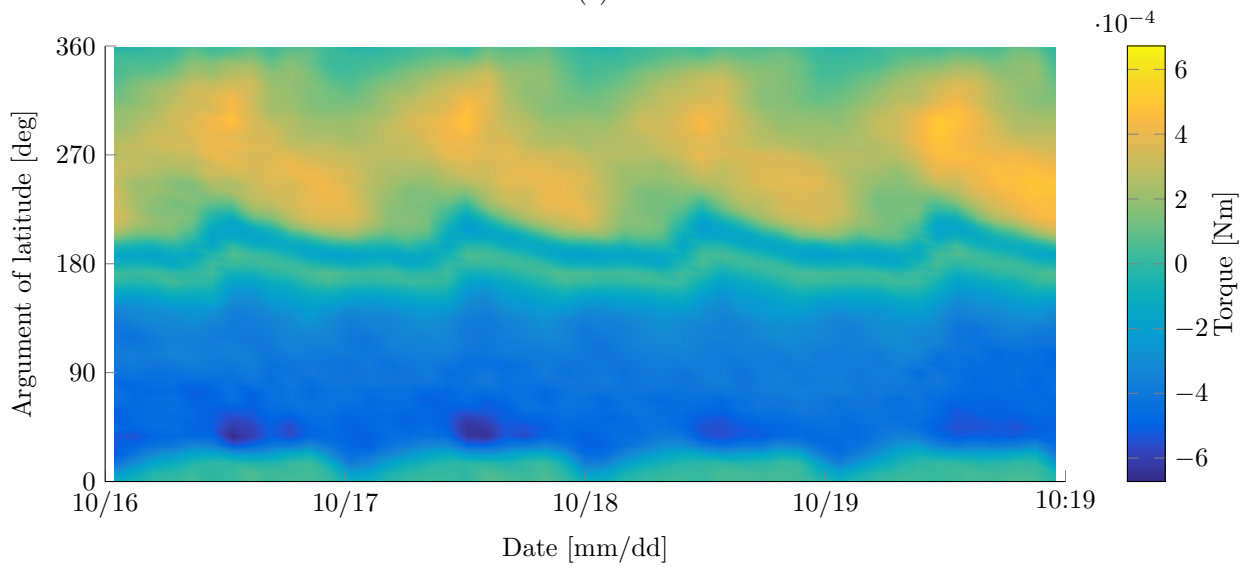
Faculty of Aerospace Engineering, Delft University of Technology, Delft, The Netherlands

B. Fritsche

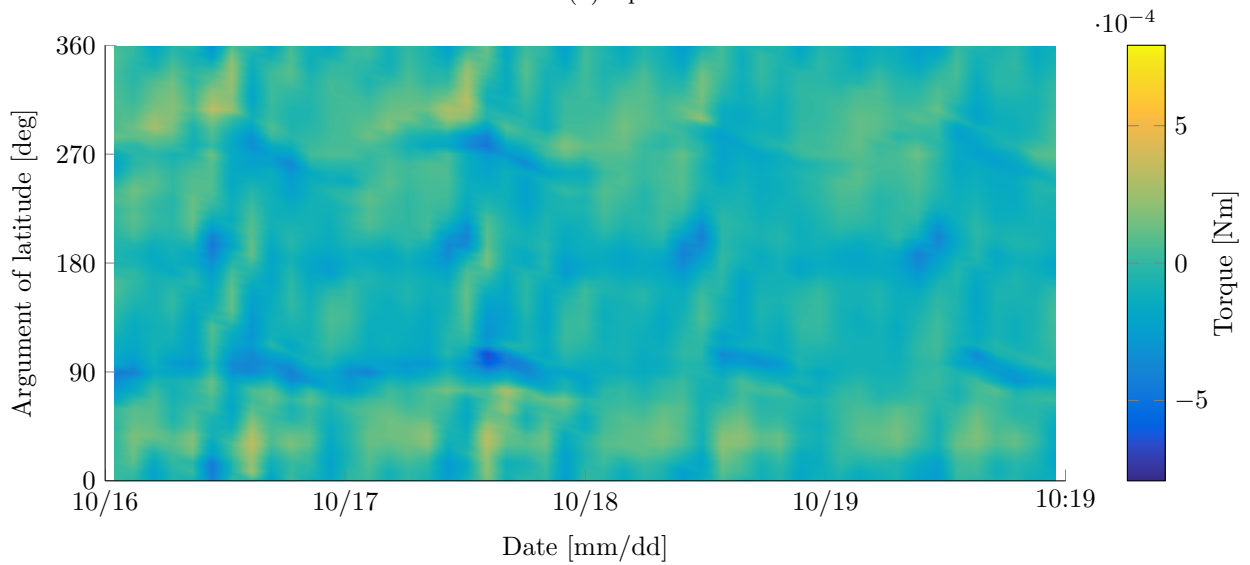
Hyperschall Technologie Göttingen GmbH, Katlenburg-Lindau, Germany



(a) \bar{T}_{roll}

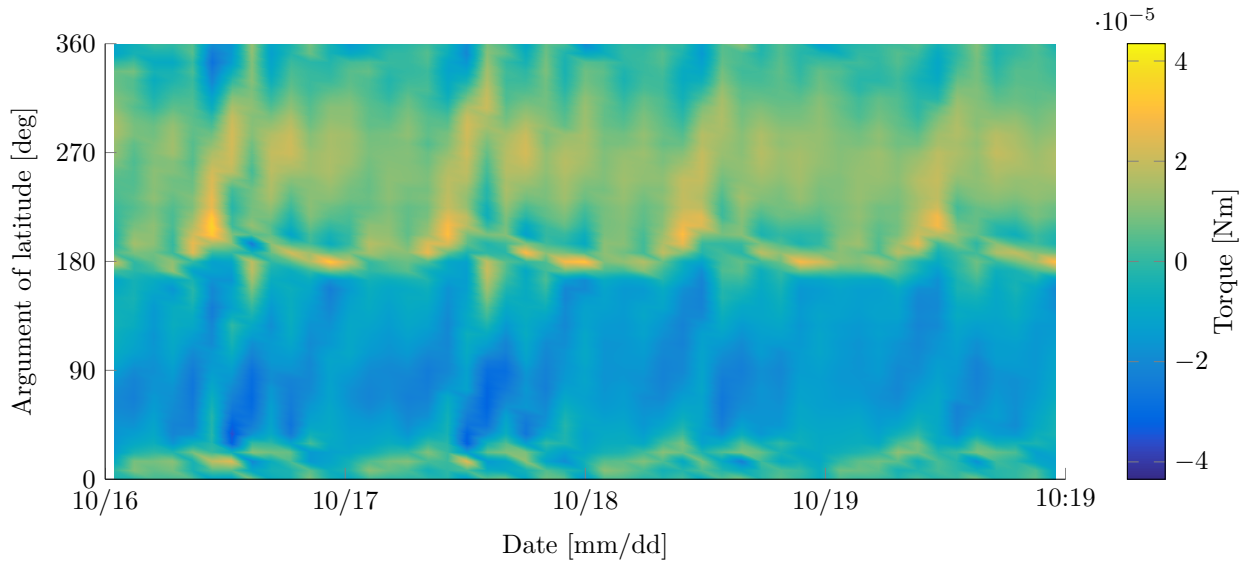


(b) \bar{T}_{pitch}

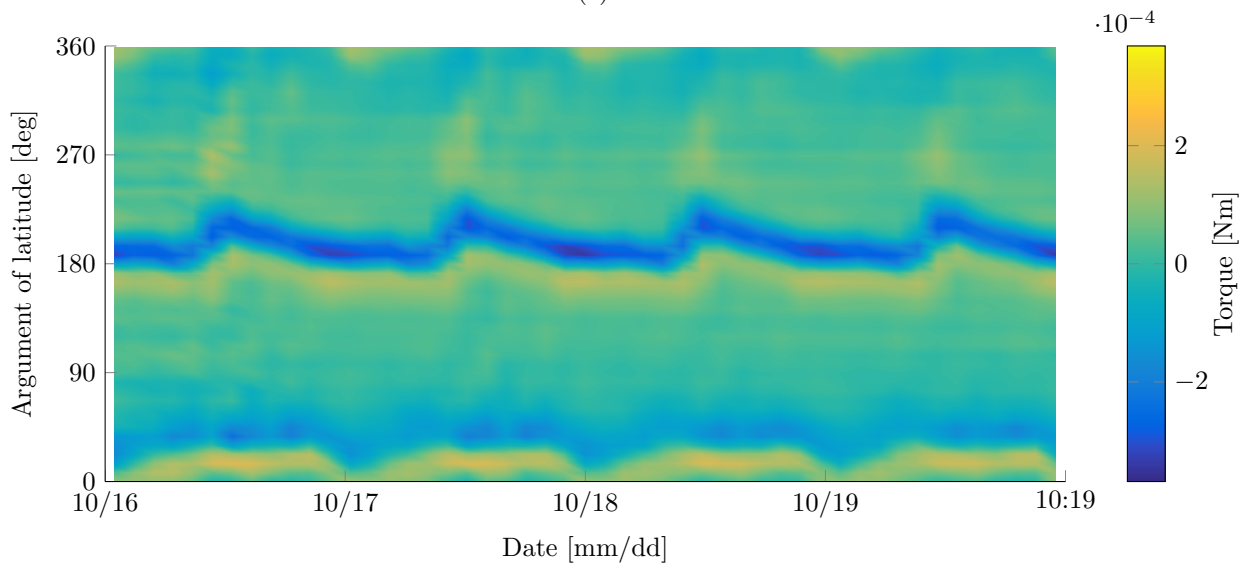


(c) \bar{T}_{yaw}

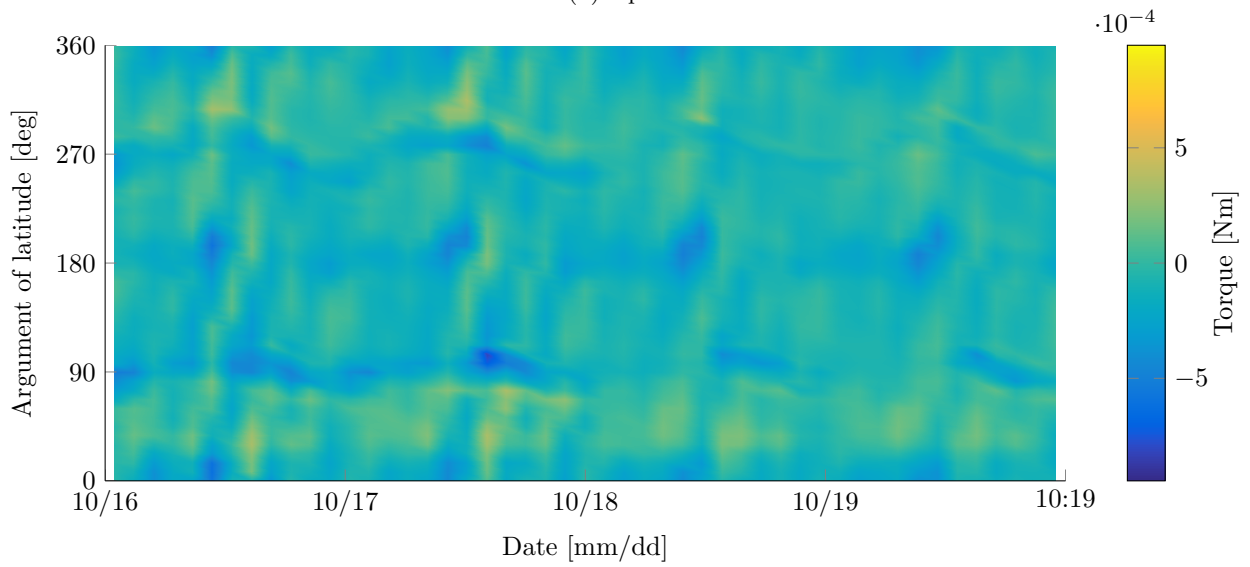
Figure 1: Total modeled torque $\bar{\mathbf{T}}$ as a function of time and argument of latitude in 2013.



(a) T_{roll}

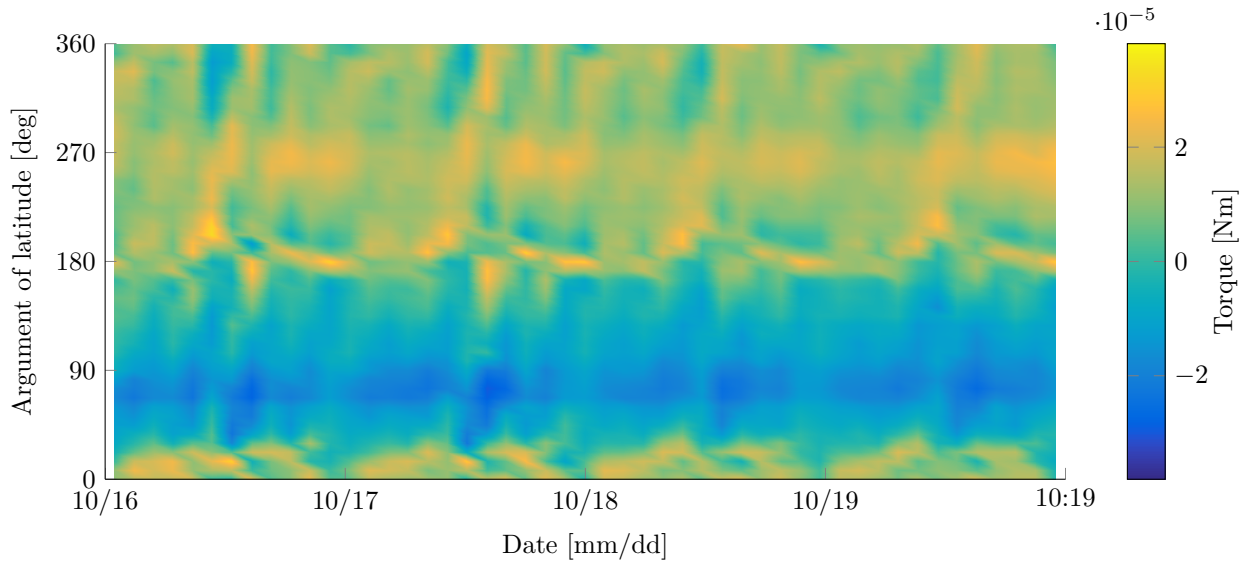


(b) T_{pitch}

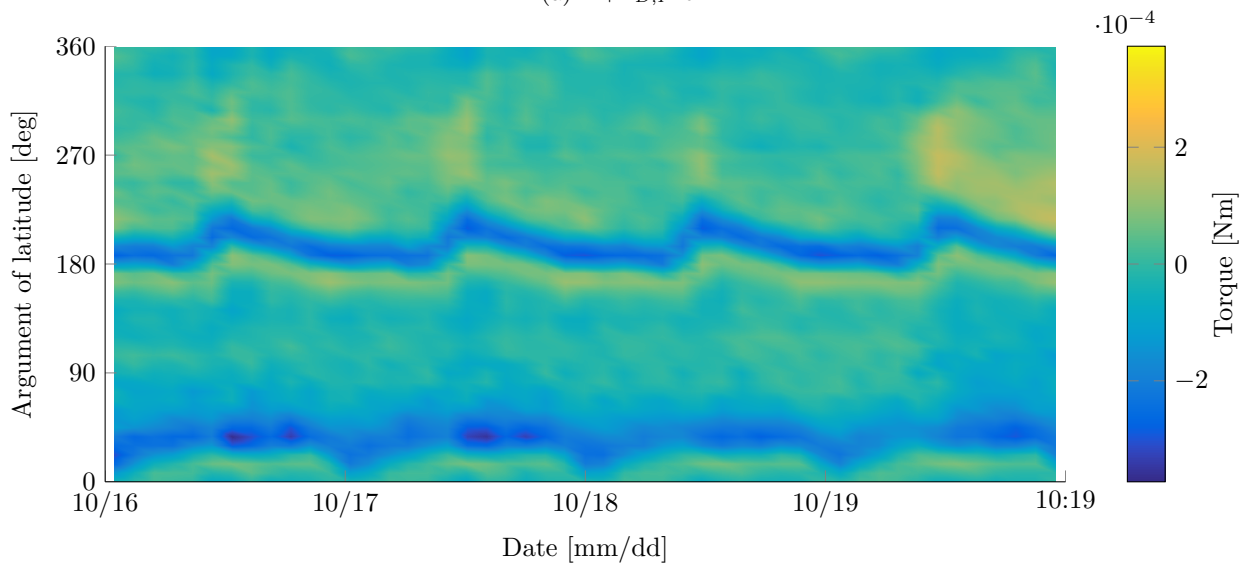


(c) T_{yaw}

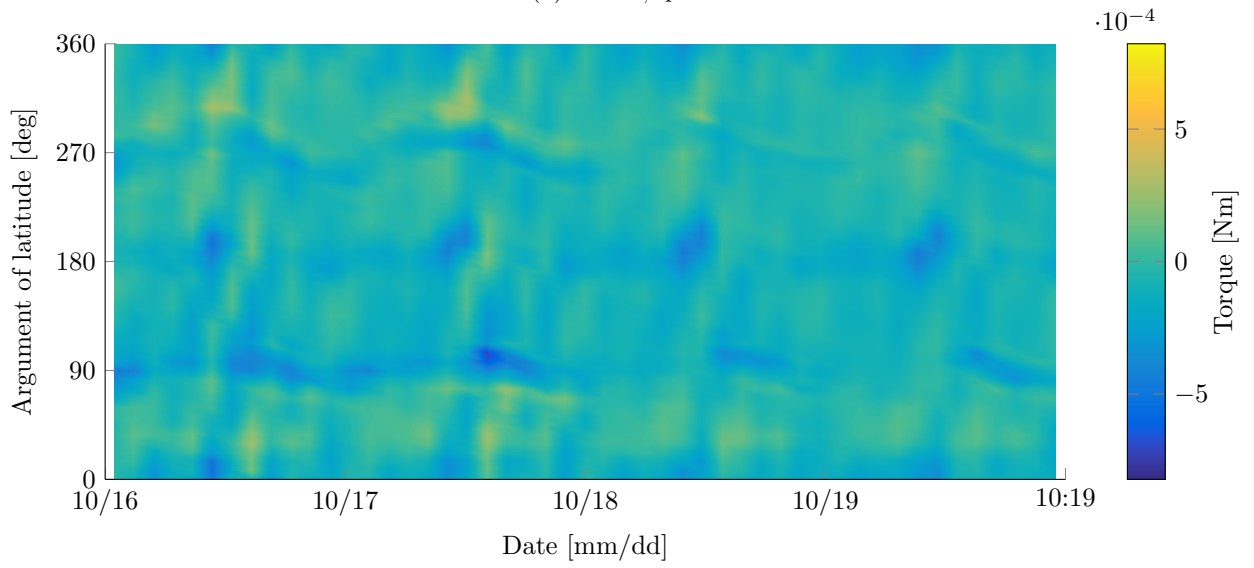
Figure 2: Measured torque \mathbf{T} as a function of time and argument of latitude in 2013.



(a) $\bar{\mathbf{T}} + \hat{\mathbf{T}}_{D,Proll}$

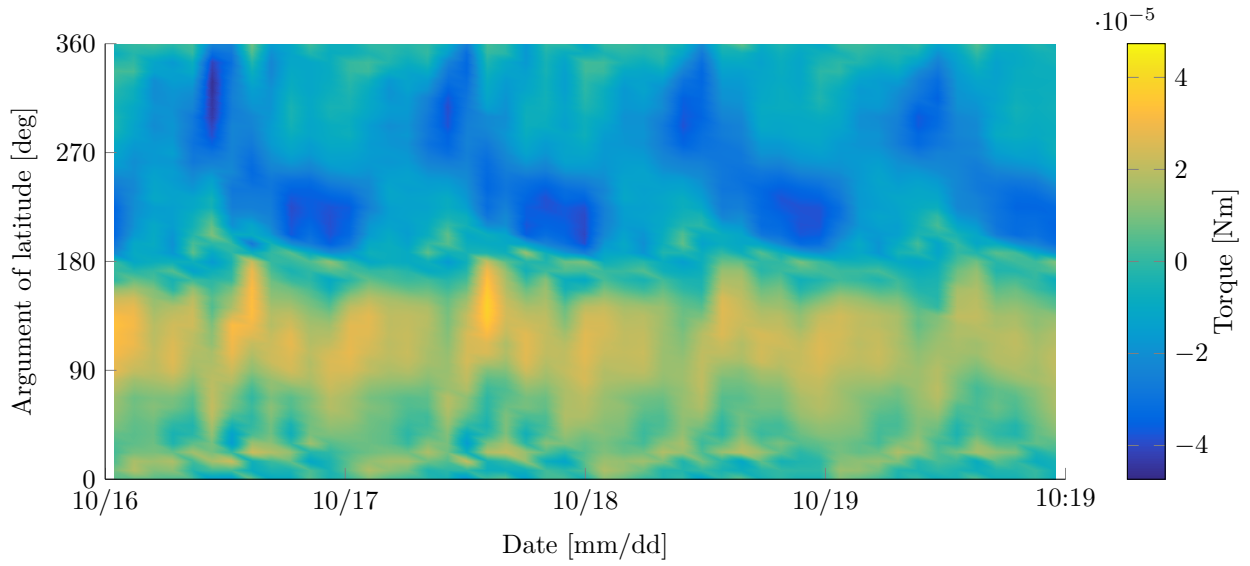


(b) $\bar{\mathbf{T}} + \hat{\mathbf{T}}_{D,Ppitch}$

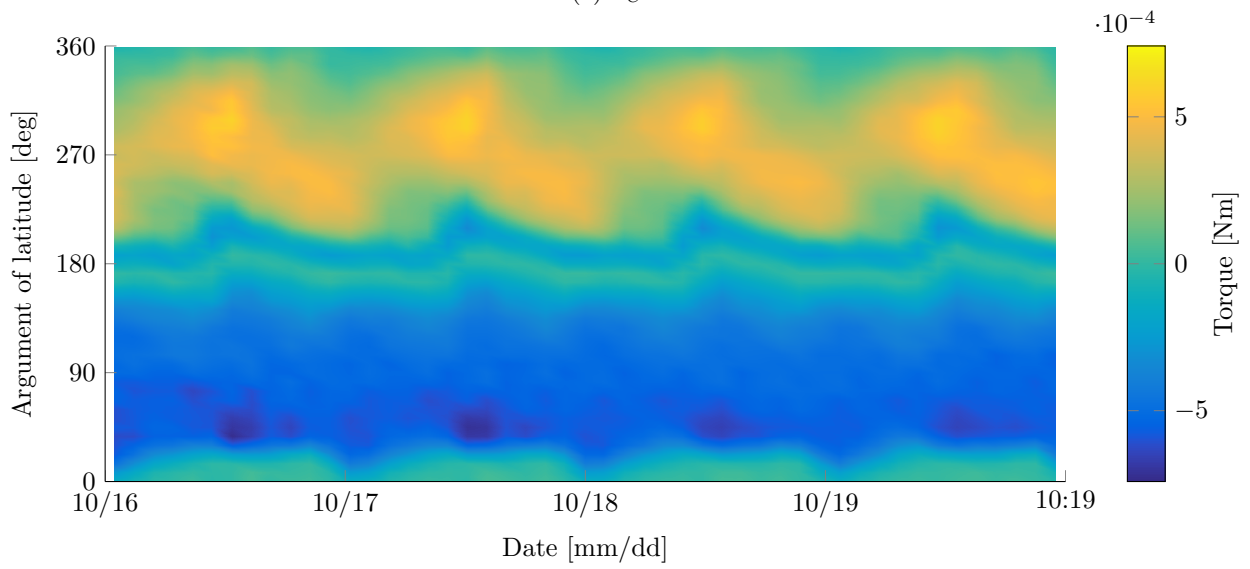


(c) $\bar{\mathbf{T}} + \hat{\mathbf{T}}_{D,Pyaw}$

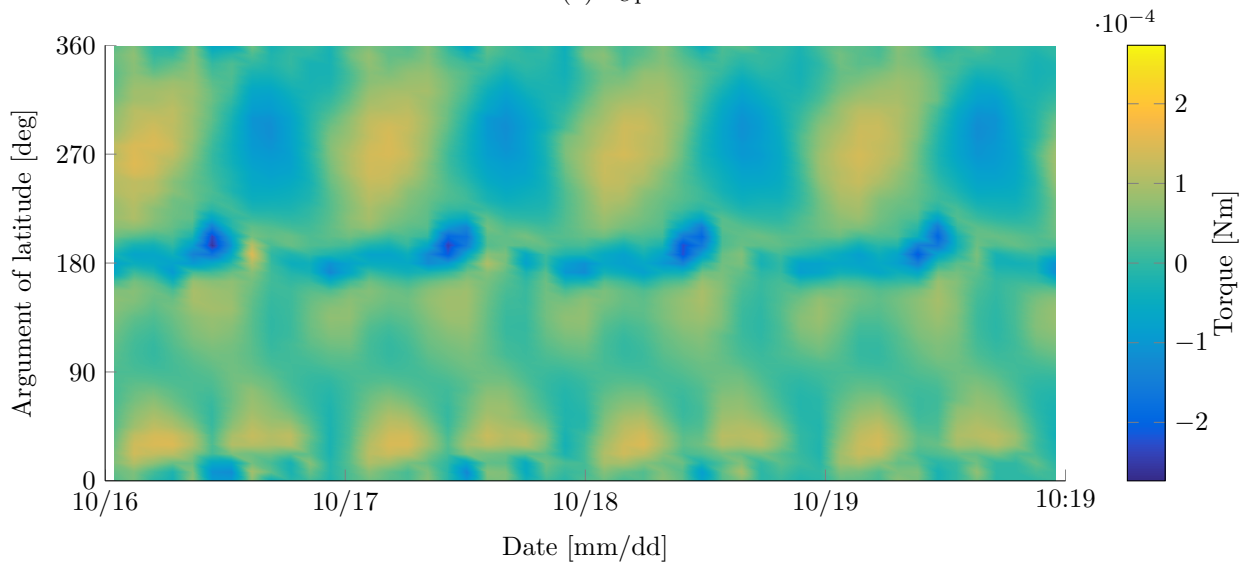
Figure 3: Total modeled torque $\bar{\mathbf{T}}$, and fitted payload dipole torque $\hat{\mathbf{T}}_{D,P}$ as a function of time and argument of latitude in 2013.



(a) $\bar{\mathbf{T}}_{C\text{roll}}$

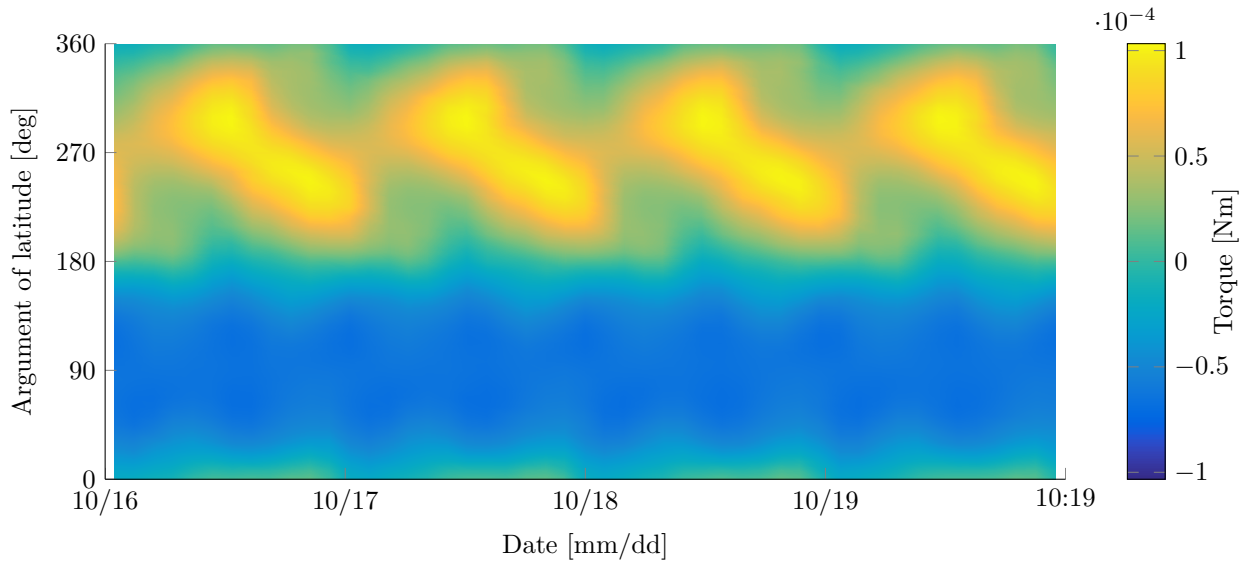


(b) $\bar{\mathbf{T}}_{C\text{pitch}}$

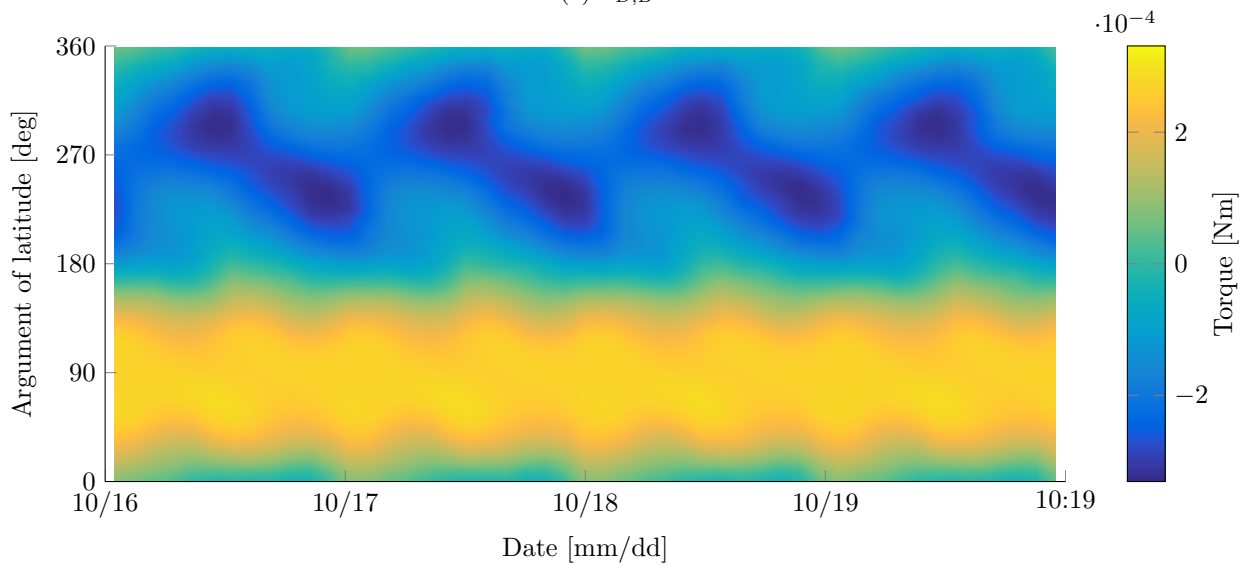


(c) $\bar{\mathbf{T}}_{C\text{yaw}}$

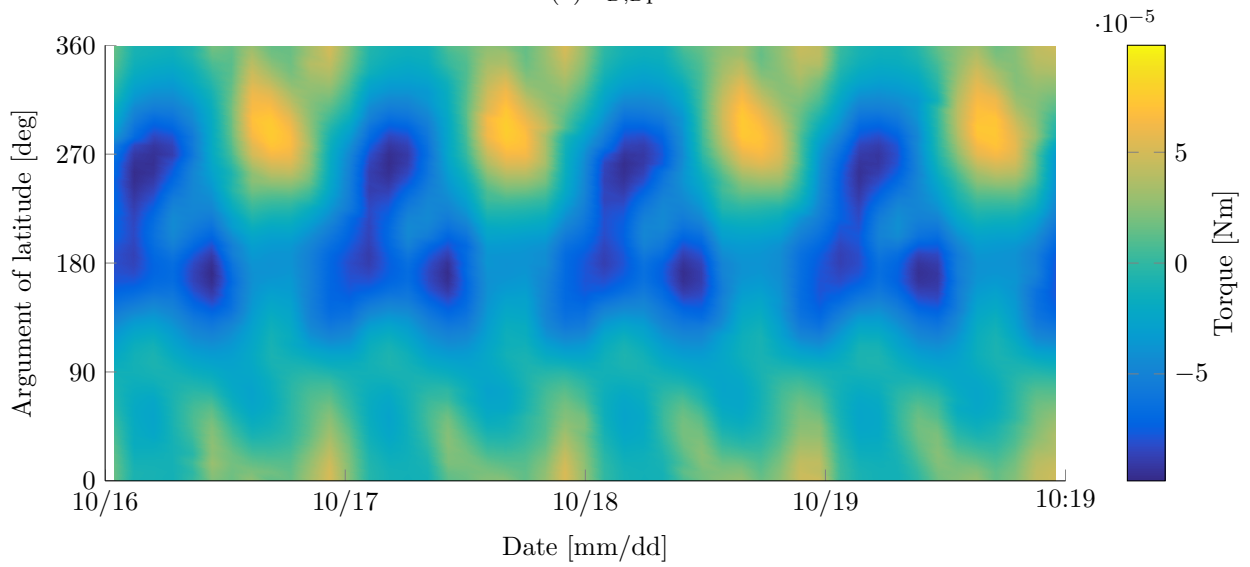
Figure 4: Magnetic control torque $\bar{\mathbf{T}}_C$ as a function of time and argument of latitude in 2013.



(a) $\bar{\mathbf{T}}_{D,B\text{roll}}$

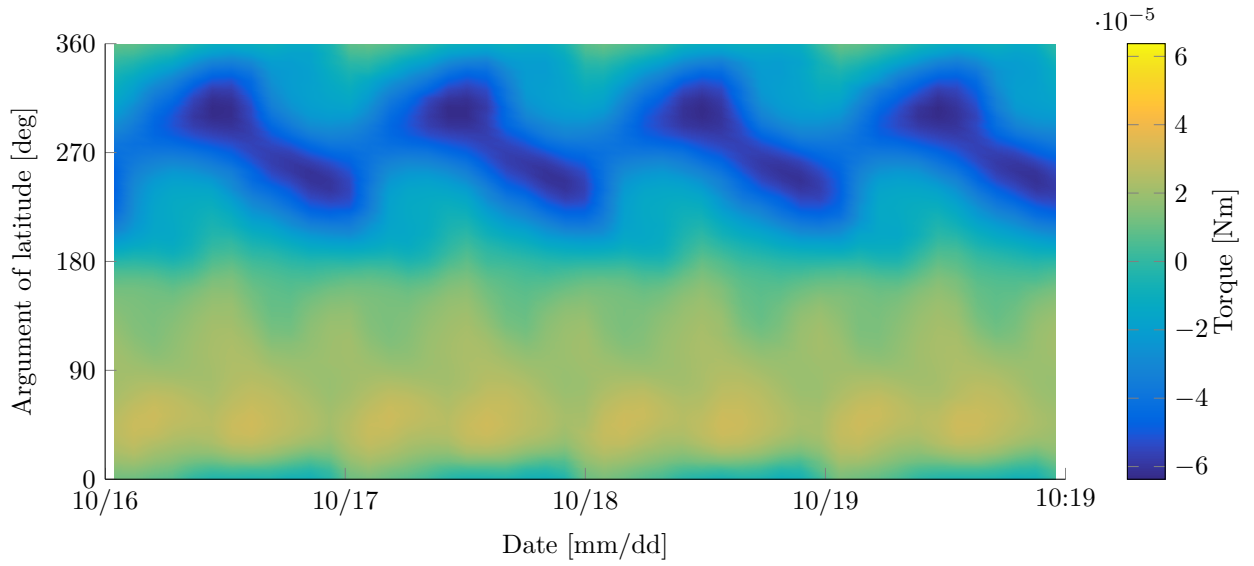


(b) $\bar{\mathbf{T}}_{D,B\text{pitch}}$

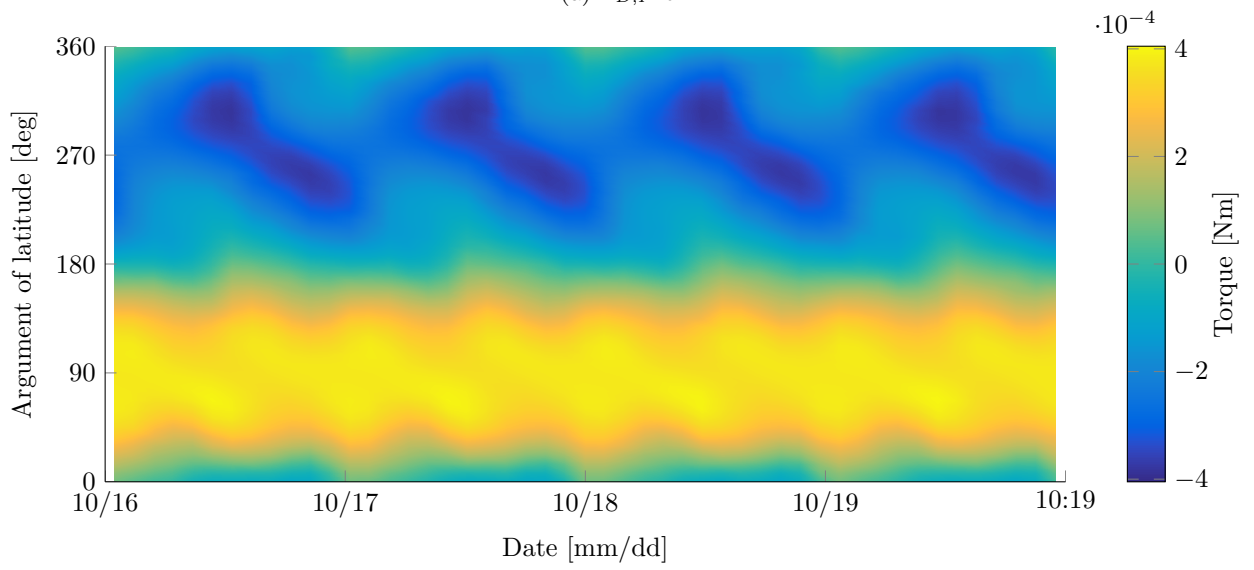


(c) $\bar{\mathbf{T}}_{D,B\text{yaw}}$

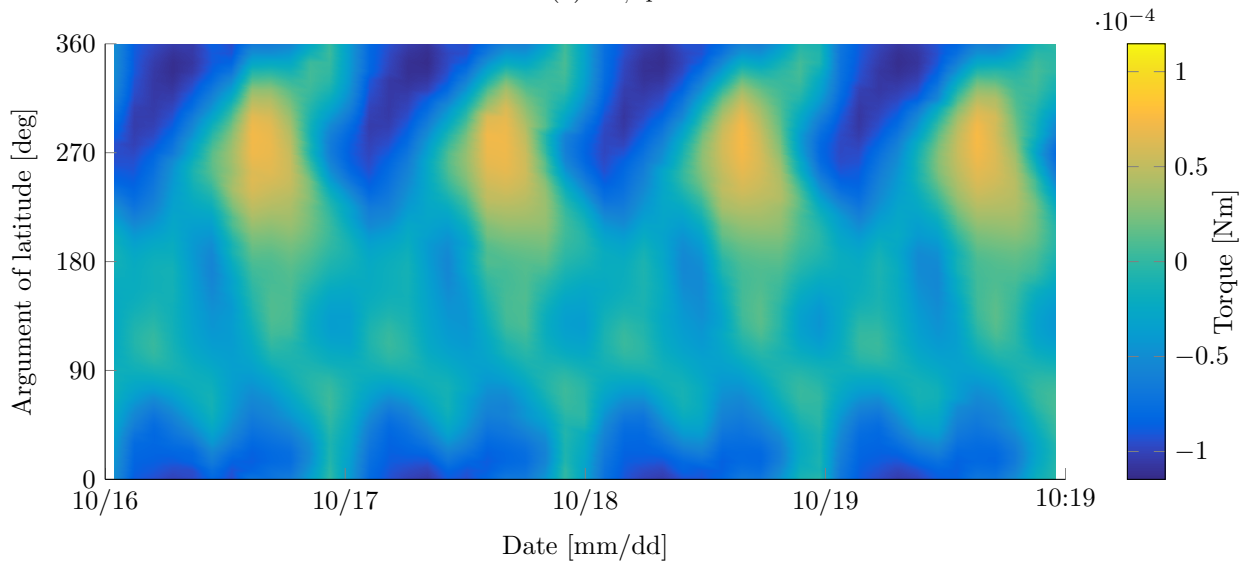
Figure 5: Residual bus dipole torque $\bar{\mathbf{T}}_{D,B}$ as a function of time and argument of latitude in 2013.



(a) $\hat{\mathbf{T}}_{D,Proll}$

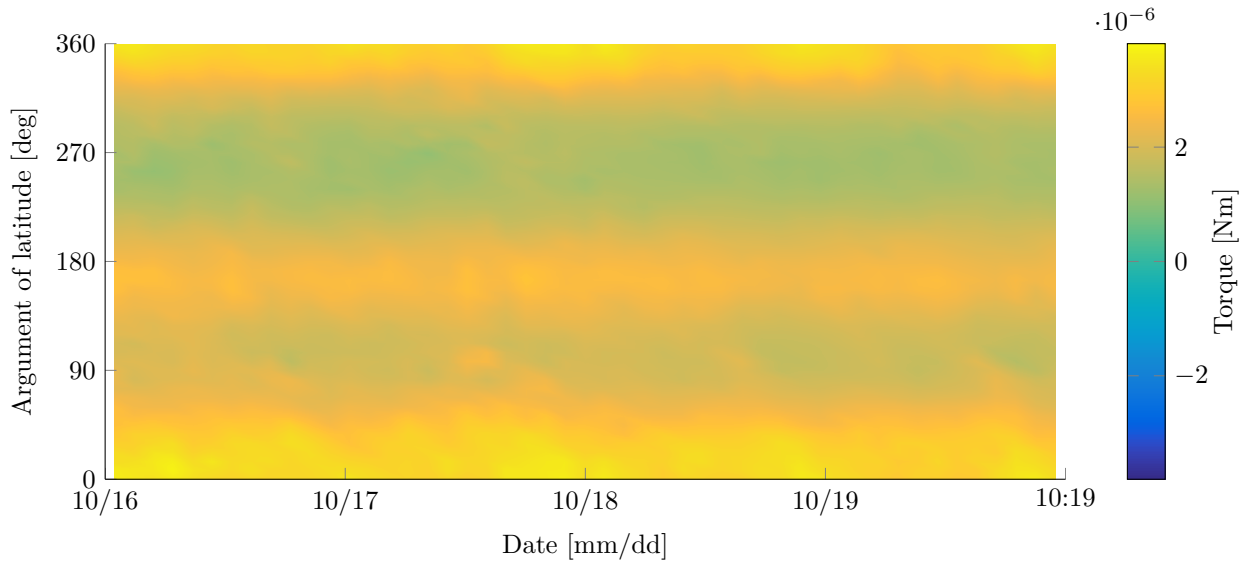


(b) $\hat{\mathbf{T}}_{D,Ppitch}$

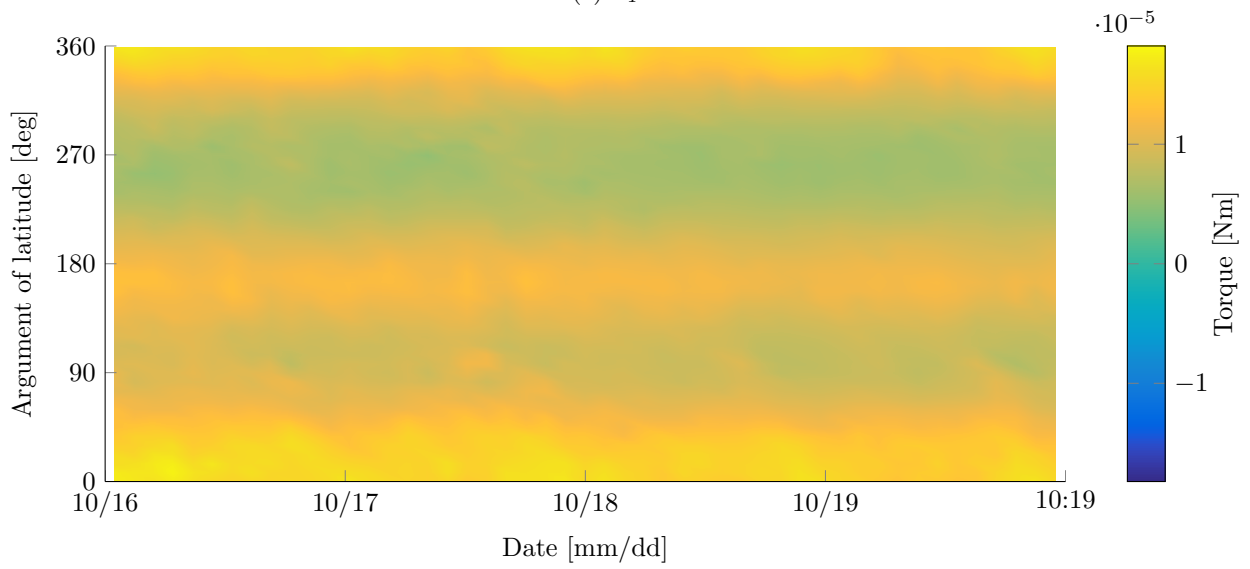


(c) $\hat{\mathbf{T}}_{D,Pyaw}$

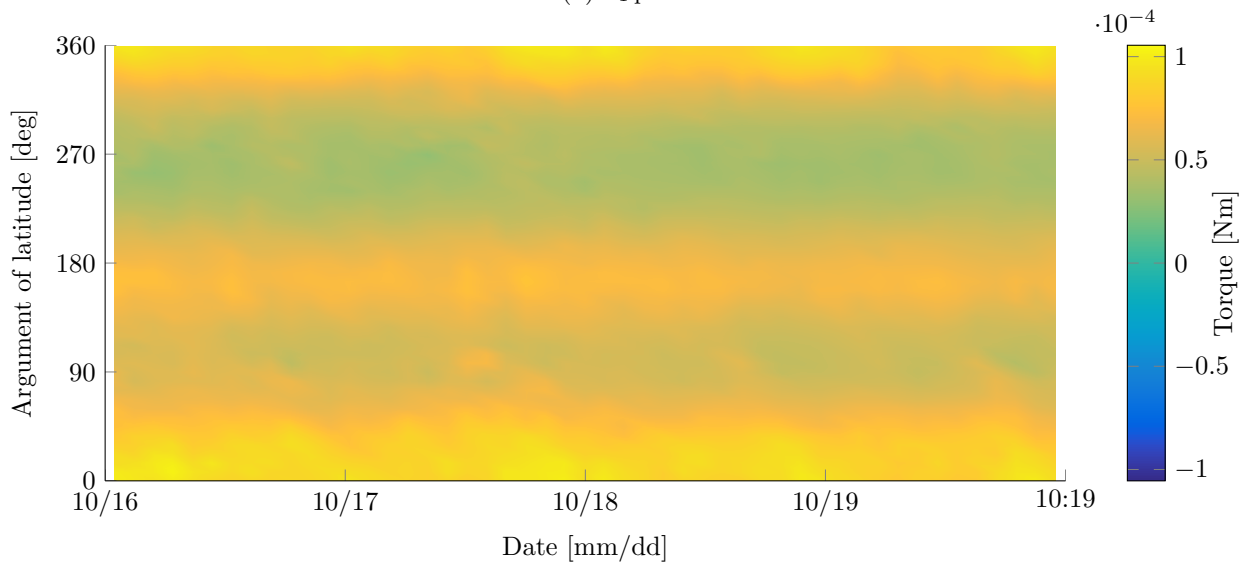
Figure 6: Fitted payload dipole torque $\hat{\mathbf{T}}_{D,P}$ as a function of time and argument of latitude in 2013.



(a) $\bar{\mathbf{T}}_{T\text{roll}}$



(b) $\bar{\mathbf{T}}_{T\text{pitch}}$



(c) $\bar{\mathbf{T}}_{T\text{yaw}}$

Figure 7: Thruster misalignment torque $\bar{\mathbf{T}}_T$ as a function of time and argument of latitude in 2013.

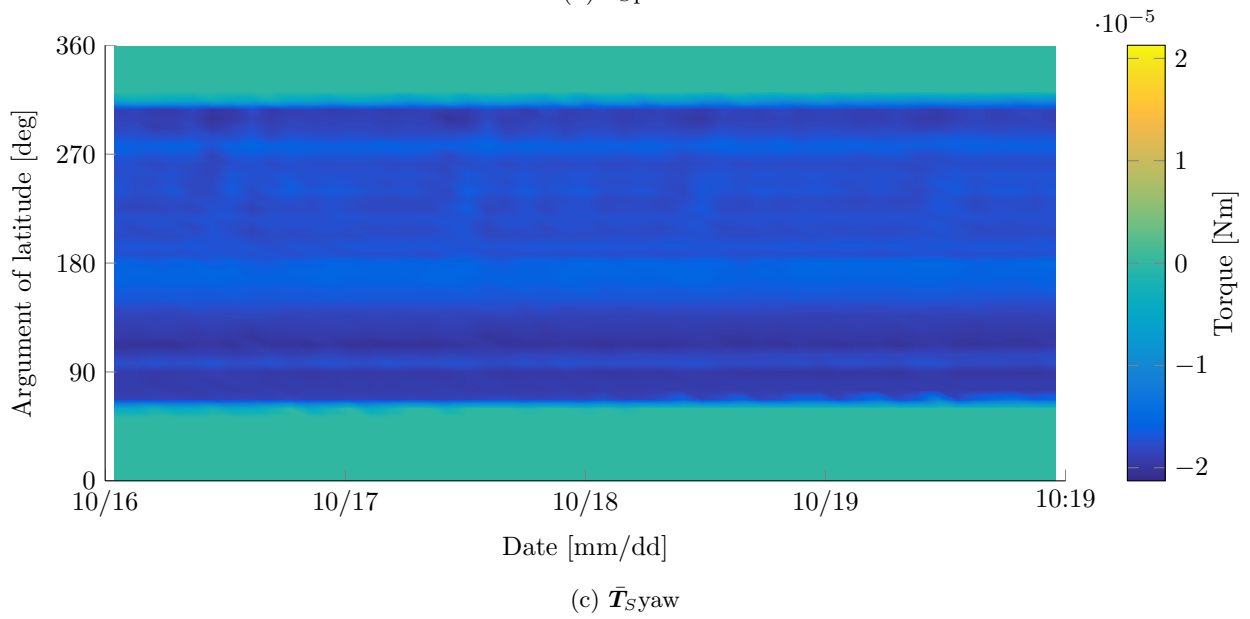
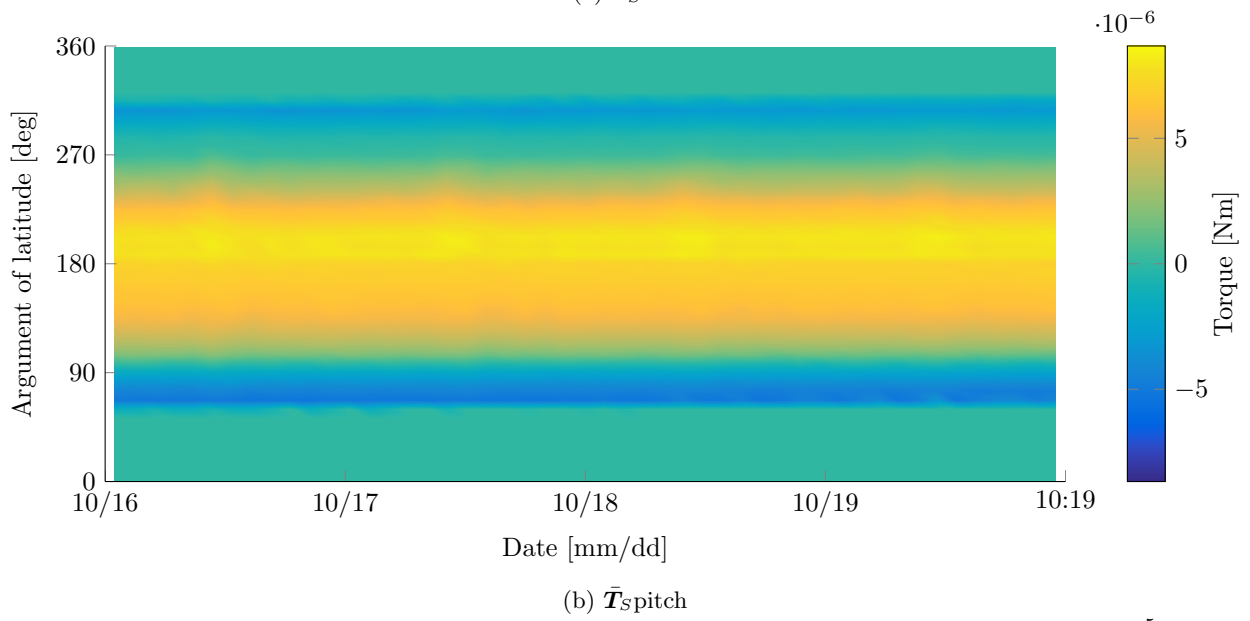
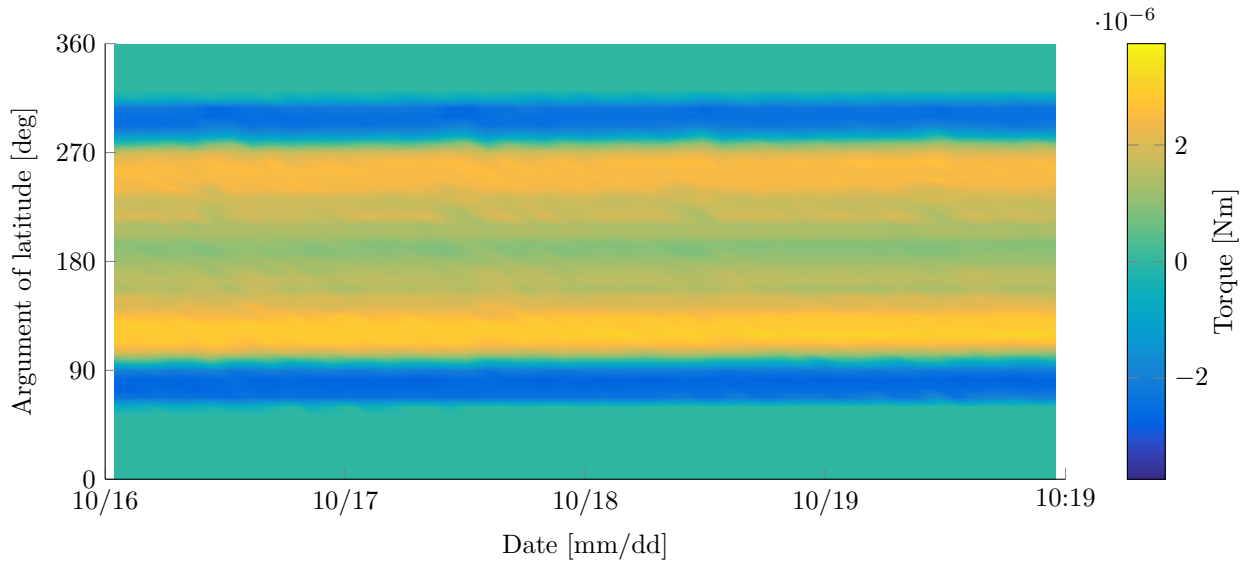
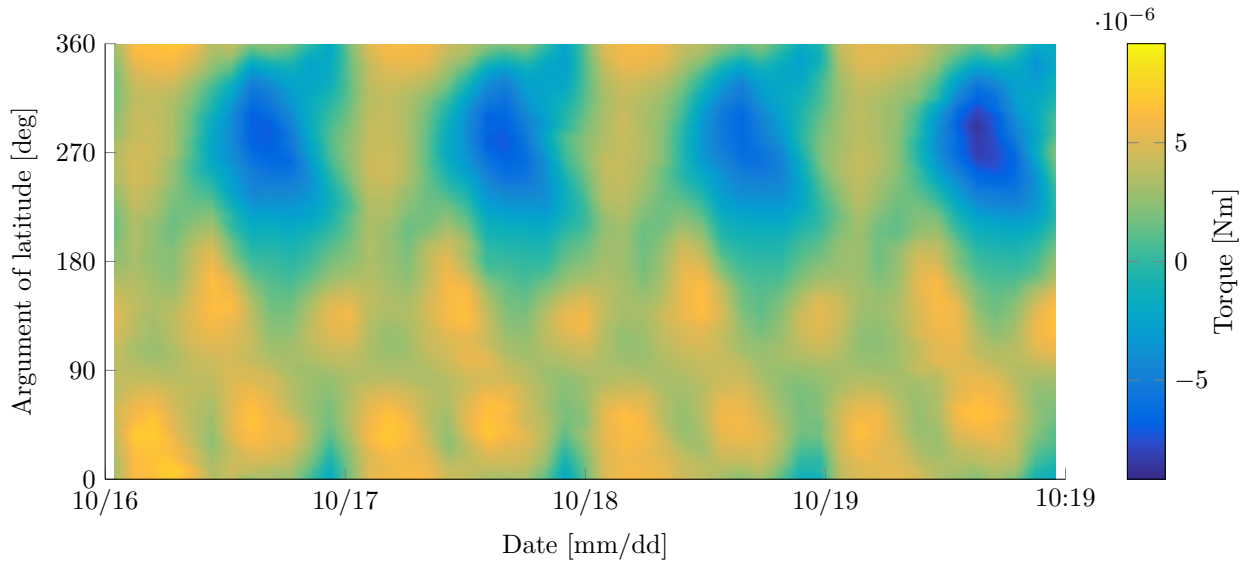
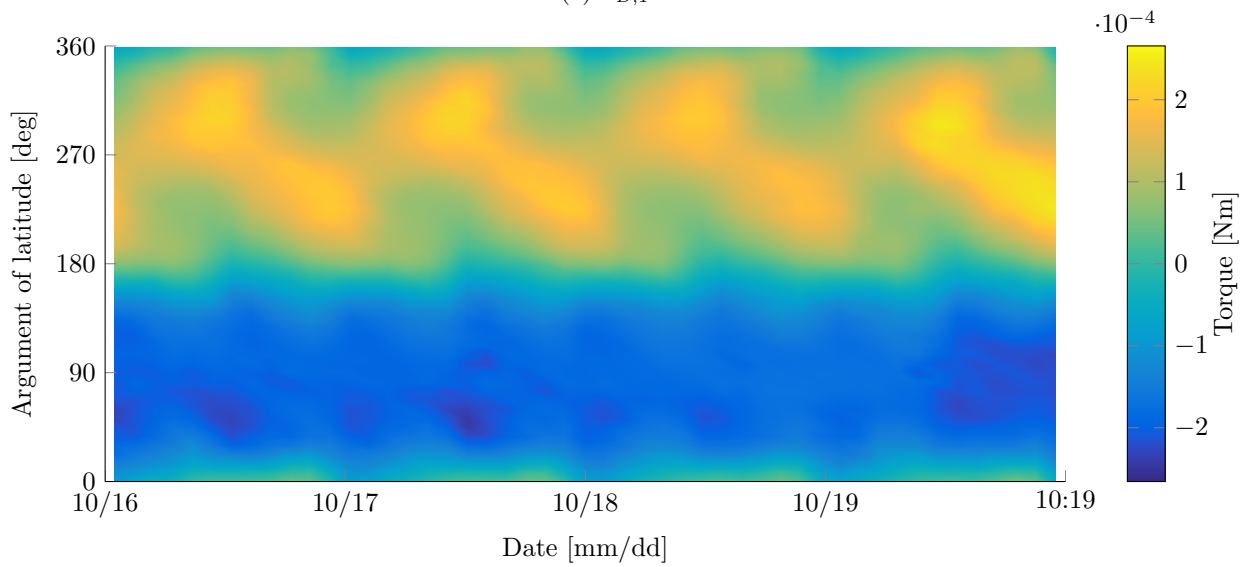


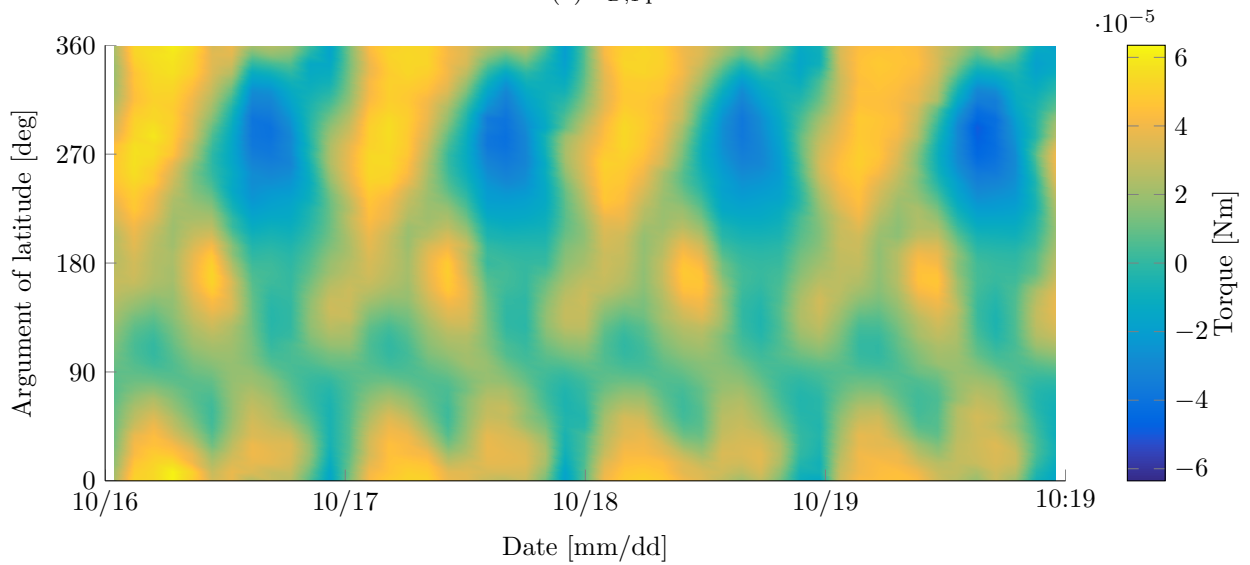
Figure 8: Solar radiation pressure torque \bar{T}_S as a function of time and argument of latitude in 2013.



(a) $\bar{\mathbf{T}}_{D,Troll}$

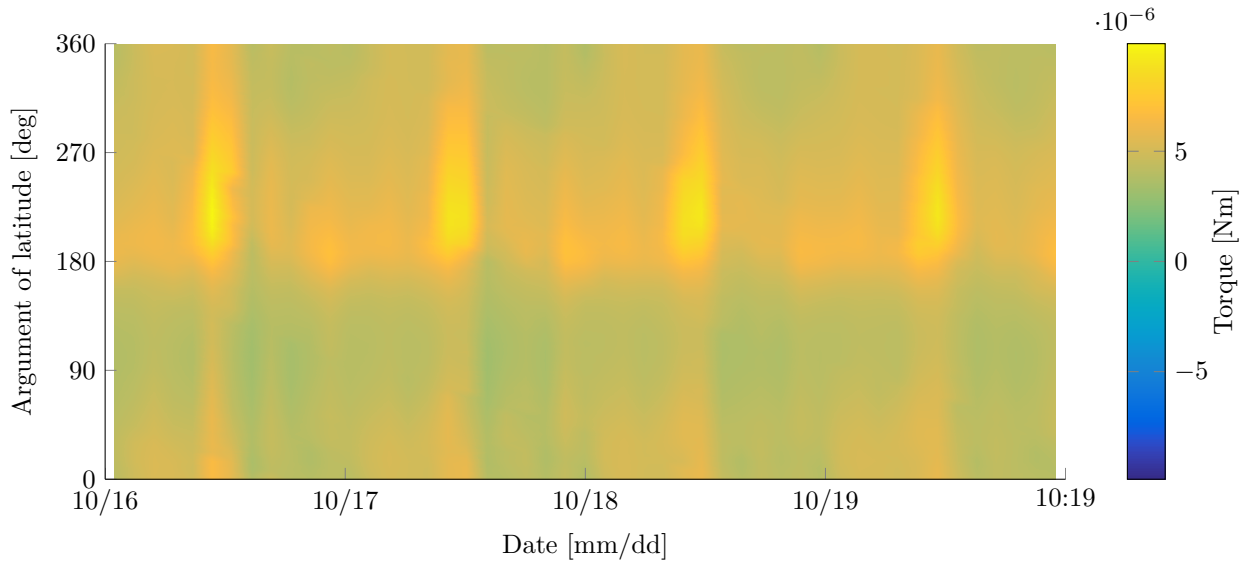


(b) $\bar{\mathbf{T}}_{D,Tpitch}$

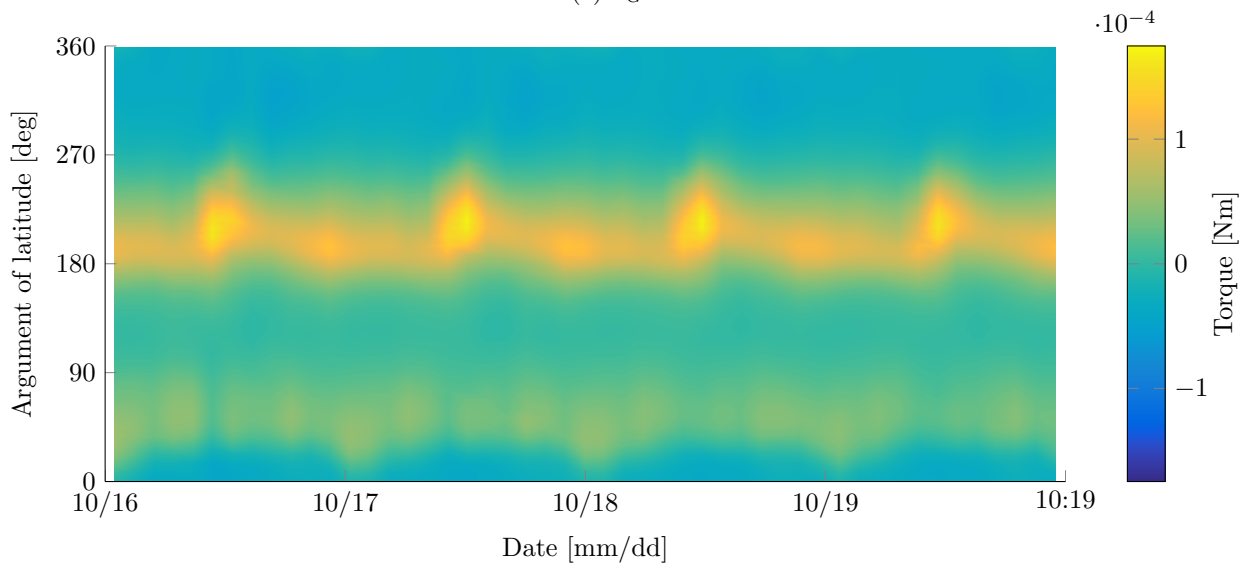


(c) $\bar{\mathbf{T}}_{D,Tyaw}$

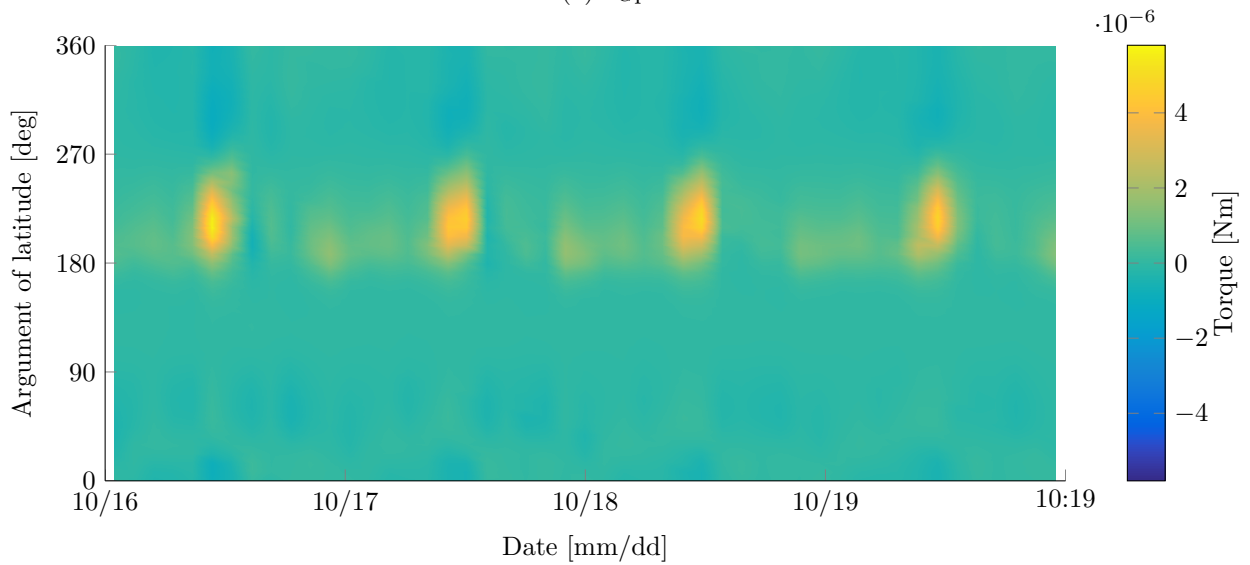
Figure 9: Thruster dipole torque $\bar{\mathbf{T}}_{D,T}$ as a function of time and argument of latitude in 2013.



(a) \bar{T}_{Groll}

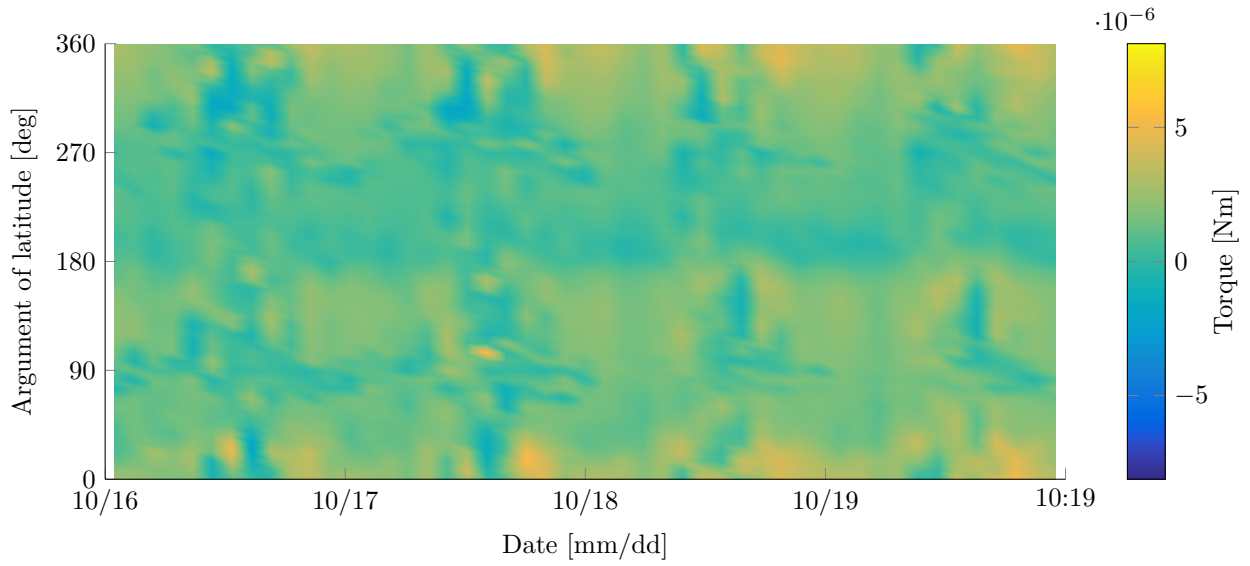


(b) \bar{T}_{Gpitch}

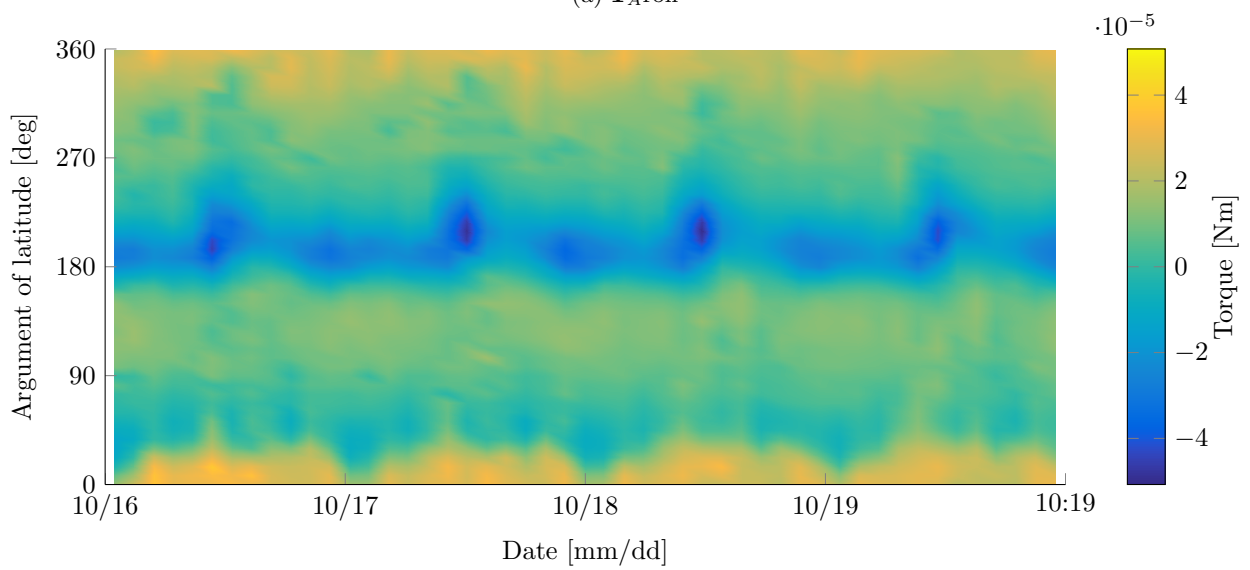


(c) \bar{T}_{Gyaw}

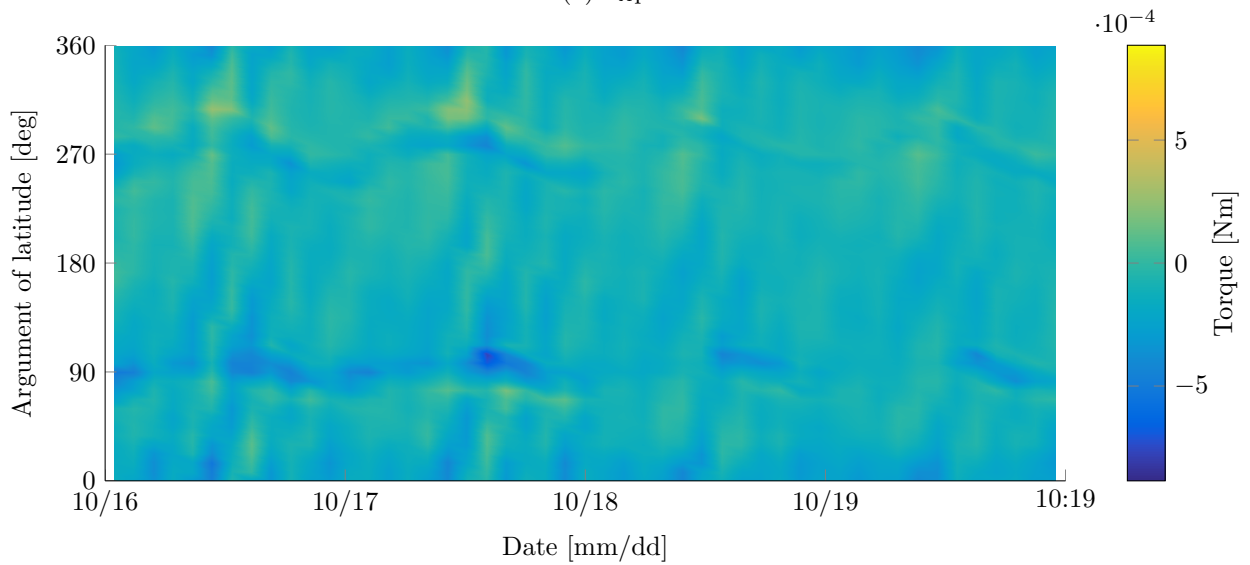
Figure 10: Gravity gradient torque \bar{T}_G as a function of time and argument of latitude in 2013.



(a) \bar{T}_{Aroll}

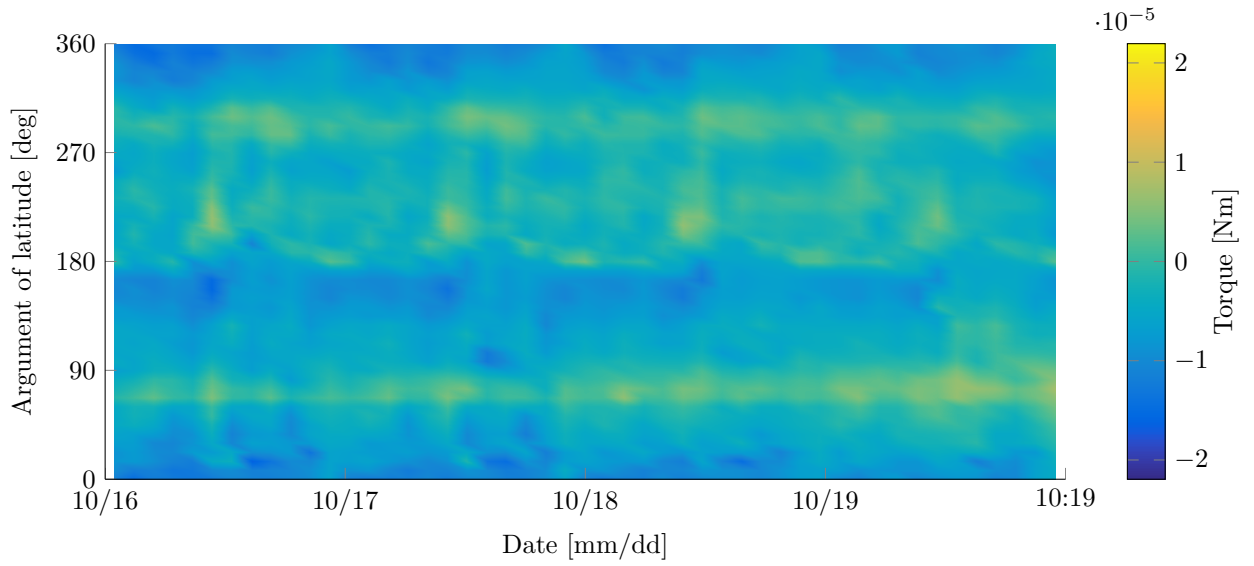


(b) \bar{T}_{Apitch}

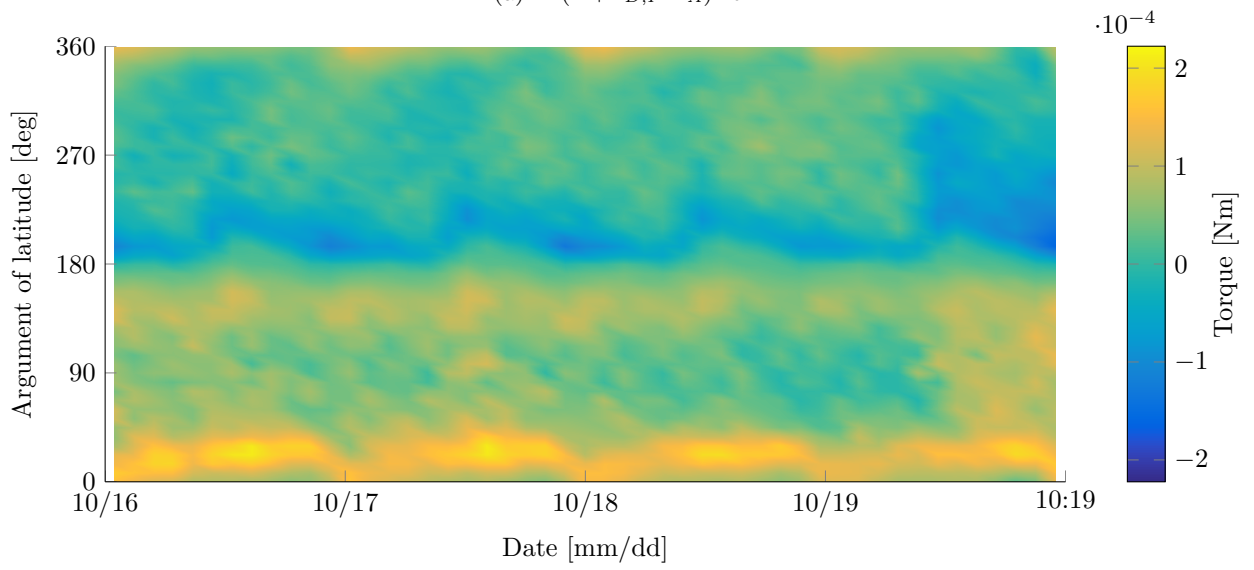


(c) \bar{T}_{Ayaw}

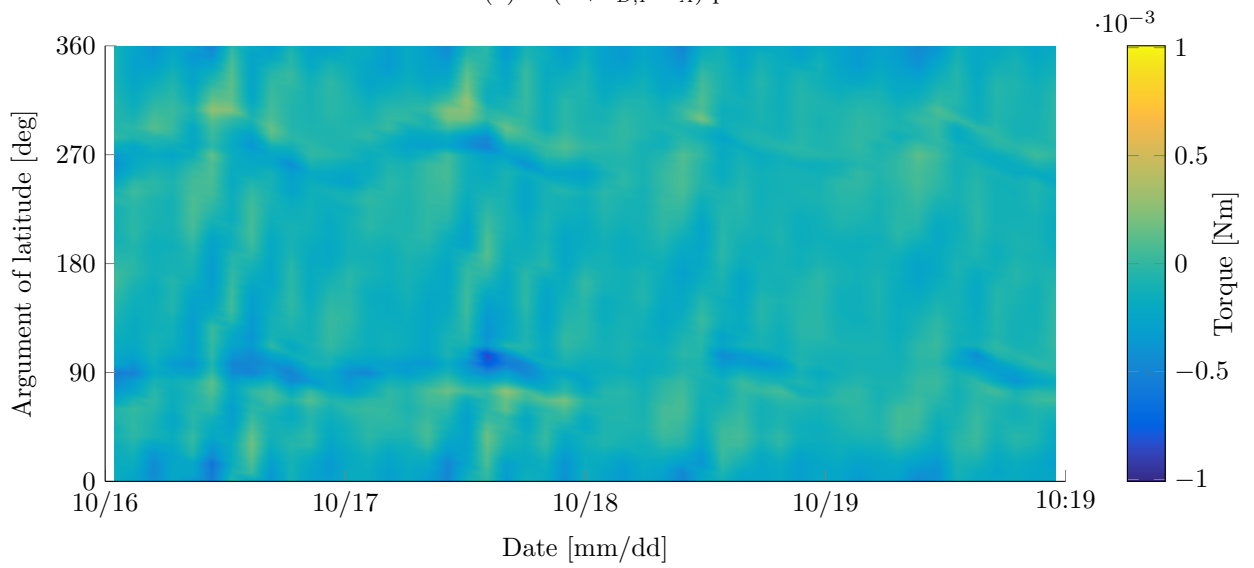
Figure 11: Aerodynamic torque \bar{T}_A as a function of time and argument of latitude in 2013.



(a) $\mathbf{T} - (\bar{\mathbf{T}} + \hat{\mathbf{T}}_{D,P} - \bar{\mathbf{T}}_A)$ roll



(b) $\mathbf{T} - (\bar{\mathbf{T}} + \hat{\mathbf{T}}_{D,P} - \bar{\mathbf{T}}_A)$ pitch



(c) $\mathbf{T} - (\bar{\mathbf{T}} + \hat{\mathbf{T}}_{D,P} - \bar{\mathbf{T}}_A)$ yaw

Figure 12: Measured torque \mathbf{T} , total modeled torque $\bar{\mathbf{T}}$, fitted payload dipole torque $\hat{\mathbf{T}}_{D,P}$, and aerodynamic torque $\bar{\mathbf{T}}_A$ as a function of time and argument of latitude in 2013.